Carbon-13 and Oxygen-17 Chemical Shifts, ($^{16}O/^{18}O$) Isotope Effects on ^{13}C Chemical Shifts, and Vibrational Frequencies of Carbon Monoxide in Various Solvents and of the Fe−C−O Unit in Carbonmonoxy Heme Proteins and Synthetic Model Compounds

Charalampos G. Kalodimos,[†] Ioannis P. Gerothanassis,*[,†] Roberta Pierattelli,[‡] and Bernard Ancian[§,||]

Department of Chemistry, Section of Organic Chemistry and Biochemistry, University of Ioannina, Ioannina GR-45110, Greece, Department of Chemistry, University of Florence, Via G. Capponi 7, 50121 Florence, Italy, Department of Chemistry, Université Paris 7—Denis Diderot, 2 Place Jussieu, 75251 Paris Cedex 05, and Bruker (UMR 50), Buroparc 1, 3 Avenue du Général de Gaulle, 91090 Lisses, France

Received December 10, 1998

^{13}C shieldings, $\delta(^{13}C)$, ^{17}O shieldings, $\delta(^{17}O)$, and ^{18}O isotope effects on ^{13}C shieldings, $^1\Delta^{13}C(^{18}O/^{16}O)$, of carbon monoxide (99.7% ^{13}C, 0.9% ^{17}O, and 11.8% ^{18}O enriched) in a variety of solvents and of the Fe−C−O unit of several carbonmonoxy hemoprotein models with varying polar and steric effects of the distal organic superstructure and constraints of the proximal side are reported. This enables, first, comparisons with hemoproteins, C−O vibrational frequencies, ν(C−O), and X-ray structural data to be made; second, to investigate whether polarizable CO is an adequate model for distal ligand effects in carbonmonoxy heme proteins and synthetic model compounds; third, to investigate the effect of electronic perturbation within the heme pocket and pocket deformation on $\delta(^{13}C)$, $\delta(^{17}O)$, $^1\Delta^{13}C(^{18}O/^{16}O)$, and ν(C−O). A variety of solvents with varying dielectric constants and solvation abilities appears to have negligible effect on $\delta(^{17}O)$, $\delta(^{13}C)$, and $^1\Delta^{13}C(^{18}O/^{16}O)$ and little direct effect on ν(C−O) of dissolved carbon monoxide. On the contrary, ^{13}C and ^{17}O shieldings of several carbonmonoxy hemoprotein models vary widely and an excellent correlation was found between the infrared C−O vibrational frequencies and ^{13}C shieldings and a reasonable correlation with ^{18}O isotope effects on ^{13}C shieldings. The ^{13}C shieldings of heme models cover a 4.0 ppm range which is extended to 7.0 ppm when several HbCO and MbCO species at different pHs are included. The latter were found to obey a similar linear $\delta(^{13}C)$ vs ν(C−O) relationship. ν(C−O), $\delta(^{13}C)$, and $^1\Delta^{13}C(^{18}O/^{16}O)$ parameters of heme model compounds reflect similar interaction which is primarily the modulation of π back-bonding from Fe d_π to CO π^* orbital by the distal pocket polar interactions. Our results suggest that, contrary to earlier claims, polarizable carbon monoxide is not an adequate model for distal ligand effects in carbonmonoxy hemoproteins and synthetic model compounds. Very probably this is caused by the large effect of the electric field on the back-bonding and the large polarizability of the π subsystem of the Fe−C−O unit. The ^{17}O shieldings of heme models cover a range of 17 ppm which is extended to 24 ppm when selected heme proteins are included. The lack of correlation between $\delta(^{13}C)$ and $\delta(^{17}O)$ suggests that the two probes do not reflect a similar type of electronic and structural perturbation. $\delta(^{17}O)$ is not primarily influenced by the local distal field interactions and does not correlate with any single structural property of the Fe−C−O unit; however, atropisomerism and deformation of the porphyrin geometry appear to play a significant role.

Introduction

The electronic nature of the Fe−C−O unit in heme proteins and synthetic model compounds has been the subject of intensive research activities for several decades.[1−3] There has been considerable interest in investigating structure−activity relationships by using vibrational spectroscopy with particular emphasis to C−O and Fe−C stretching frequencies and Fe−C−O bending deformation.[4−7] More recently, considerable new information was obtained by the use of ^{13}C, ^{17}O, and ^{57}Fe NMR both in solution and in the solid state.[8−12] As pointed out by Oldfield and collaborators,[11a] there are at least fourteen independent NMR

* To whom correspondence should be addressed. Tel.: +33 0651-98389. Fax: +33 0651-45840. E-mail: igeroth@cc.uoi.gr.
[†] University of Ioannina.
[‡] University of Florence.
[§] Université Paris 7.
[||] Bruker (UMR 50).

(1) (a) Collman, J. P. *Inorg. Chem.* **1997**, *36*, 5145−5155. (b) Perutz, M. F.; Fermi, G.; Luisi, B.; Shaanan, B.; Liddington, R. C. *Acc. Chem. Res.* **1987**, *20*, 309−321.
(2) Momenteau, M.; Reed, C. A. *Chem. Rev.* **1994**, *94*, 659−698.
(3) (a) Springer, B. A.; Sligar, S. G.; Olson, J. S.; Phillips, G. N., Jr. *Chem. Rev.* **1994**, *94*, 699−714. (b) Sage, J. T. *J. Biol. Inorg. Chem.* **1997**, *2*, 537−543. (c) Olson, J. S.; Phillips, G. N., Jr. *J. Biol. Inorg. Chem.* **1997**, *2*, 544−552.
(4) (a) Li, X.-Y.; Spiro, T. G. *J. Am. Chem. Soc.* **1988**, *110*, 6024−6033. (b) Ray, G. B.; Li, X.-Y.; Ibers, J. A.; Sessler, J. L.; Spiro, T. G. *J. Am. Chem. Soc.* **1994**, *116*, 162−176.
(5) (a) Oldfield, E.; Guo, K.; Augspurger, J. D.; Dykstra, C. E. *J. Am. Chem. Soc.* **1991**, *113*, 7537−7541. (b) Cameron, A. D.; Smerdon, S. J.; Wilkinson, A. J.; Habash, J.; Helliwell, R.; Li, T.; Olson, J. S. *Biochemistry* **1993**, *32*, 13061−13070. (c) Li, T.; Quillin, M. L.; Phillips, G. N., Jr.; Olson, J. S. *Biochemistry* **1994**, *33*, 1433−1446.
(6) (a) Lim, M.; Jackson, T. A.; Anfinrud, P. A. *Science* **1995**, *269*, 962−966. (b) Lim, M.; Jackson, T. A.; Anfinrud, P. A. *J. Biol. Inorg. Chem.* **1997**, *2*, 531−536.
(7) Potter, W. T.; Hazzard, J. H.; Choc, M. J.; Tucker, M. P.; Caughey, W. S. *Biochemistry* **1990**, *29*, 6283−6295.

10.1021/ic9814165 CCC: $18.00
Published on Web 09/20/1999

parameters that can be used to describe the nature of the Fe−C−O fragment.

Park et al.[11a] first noted linear correlations between ν(C−O) vibrational frequencies, ^{13}C and ^{17}O chemical shifts and ^{17}O quadrupole coupling constants in various carbonmonoxy heme proteins. Augspurger et al.[13] later proposed a model for these experimental correlations. In their model, the dependence of ν(C−O), δ(^{13}C), and δ(^{17}O) on an external uniform field, a field gradient, and a potential due to a dipole for an isolated CO molecule was calculated at the Hartree−Fock level. It was suggested that polarizable CO is an adequate model for distal ligand effects in carbonmonoxy heme proteins, and that changes in both ^{13}C and ^{17}O chemical shifts are direct consequence of the imposed electrical perturbation, while changes in the vibrational frequency are due to changes in the bond length brought about by the external field. The signs of the observed NMR and IR frequency shifts are rather well reproduced by calculation, although the magnitudes are overestimated.[13]

De Dios and Earle[14] investigated the effects of a uniform external electric field applied along the Fe−C−O axis on δ(^{13}C), δ(^{17}O), and ν(C−O) by using a model consisting of Fe^{+2} octahedrally coordinated to five negative point charges and a CO molecule. Both δ(^{17}O) and ν(C−O) were found to increase as the electric field is increased while δ(^{13}C) changes in the opposite direction. Furthermore, changes in δ(^{13}C) and δ(^{17}O) vs ν(C−O) in the presence of a point charge of various magnitudes were also investigated.

Kushkuley and Stavrov[15] performed quantum chemical calculation, vibronic theory of activation, and the London−Pople approach to investigate the dependence of ν(C−O), δ(^{17}O), and ^{17}O nuclear quadrupole coupling constant (NQCC) on the distortion of the porphyrin ring and geometry of the CO coordination, changes in the Fe−C and Fe−N_{Im} distances, magnitude of the Fe displacement from the porphyrin plane, and presence of charged groups in the heme environment. It was shown that only the electrostatic interactions can cause the variation of all these parameters and the heme distortions could modulate this variation.

More recently McMahon et al.[12a] presented a unified model based on δ(^{13}C), δ(^{17}O), δ(^{57}Fe), ^{17}O nuclear quadrupole couplings, ^{57}Fe Mössbauer quadrupole splitting, and ν(C−O). It was suggested that the above spectroscopic observables can be well accounted for in terms of a linear, untilted Fe−C−O unit under the influence of weak electrostatic fields.

Because of the general complexity of the globin and its interaction with the heme, model systems have been synthesized to probe how steric and polar interactions affect ligand binding and ultimately to elucidate important aspects of the mechanism of CO discrimination.[16] High-resolution X-ray crystal structures of several CO adducts indicate that the primary type of distortion observed upon CO binding is vertical or lateral expansion of the cap and some ruffling of the porphyrin plane.[17−20] Minimal bending or tilting of the Fe−C−O bond is observed, suggesting that the Fe−C−O bending that has been found in crystal structures of hemoproteins is rather unlikely.

In this paper, we report ^{13}C and ^{17}O shieldings, and ^{18}O isotope effects on ^{13}C shielding for carbon monoxide in a variety of solvents and for a number of hemoprotein carbonmonoxy model compounds (Figure 1) in order to investigate whether electrically perturbed carbon monoxide is a possible model for distal ligand effects in carbonmonoxy hemoproteins. Due to knowledge of seven high-resolution single-crystal X-ray structural data of six-coordinated iron porphyrins with CO, a further objective of this work was to identify changes in the ^{13}C and ^{17}O shieldings and ^{18}O isotope effects on ^{13}C shieldings of bound CO as a function of polar and steric effects of the distal organic superstructure and constraints of the proximal side. Also, it was hoped that these NMR measurements might lead to possible correlations with NMR data of heme proteins, vibrational frequencies and geometric information (e.g., the Fe−C−O bond angle and C−O bond length derived from X-ray diffraction measurements).

Experimental Section

Sample Preparation. The iron(III)-porphyrin superstructure complexes in the chloride form were synthesized and characterized by the methods described previously.[8] The complexes were treated in dichloromethane solution. After deoxygenation by flushing with pure argon, the sample was reduced to the iron(II) form using aqueous sodium dithionite solution. After separation of the two phases, the organic layer of the reduced compound was transferred under argon into a second vessel containing an excess of either 1-methylimidazole or 1,2-dimethylimidazole. The resulting powder obtained after removal of the aqueous phase and subsequent evaporation of the organic solvent was then loaded into a glass ampule, connected to a vacuum pump, and evacuated at room temperature for 3 h at a pressure of 10^{-4} Torr. The sample was dissolved in deuterated dichloromethane and transferred under argon into the NMR tube via a stainless steel tube. ^{13}CO (99.7% enriched in ^{13}C, 0.9% in ^{17}O and 11.9% in ^{18}O; Euriso-top, Group CEA (Saclay, France)) under atmospheric pressure was then introduced to the sample to form the carbonylated derivative, and the NMR tube was sealed under pressure of ∼1 atm.

(8) (a) Kalodimos, C. G.; Gerothanassis, I. P. *J. Am. Chem. Soc.* **1998**, *120*, 6407−6408. (b) Kalodimos, C. G.; Gerothanassis, I. P.; Troganis, A.; Loock, B.; Momenteau, M. *J. Biomol. NMR* **1998**, *11*, 423−435. (c) Kalodimos, C. G.; Gerothanassis, I. P.; Hawkes, G. E. *Biospectroscopy* **1998**, *4*, S57−S69.
(9) (a) Gerothanassis, I. P.; Barrie, P. J.; Momenteau, M.; Hawkes, G. E. *J. Am. Chem. Soc.* **1994**, *116*, 11944−11949. (b) Gerothanassis, I. P.; Momenteau, M.; Barrie, P. J.; Kalodimos, C. G.; Hawkes, G. E. *Inorg. Chem.* **1996**, *35*, 2674−2679.
(10) (a) Gerothanassis, I. P.; Kalodimos, C. G.; Hawkes, G. E.; Haycock, P. *J. Magn. Reson.* **1998**, *131*, 163−165. (b) Baltzer, L.; Landergren, M. *J. Am. Chem. Soc.* **1990**, *112*, 2804−2805. (c) Kalodimos, C. G.; Gerothanassis, I. P.; Rose, E.; Hawkes, G. E.; Pierattelli, R. *J. Am. Chem. Soc.* **1999**, *121*, 2903−2908.
(11) (a) Park, K. D.; Guo, K.; Adebodun, F.; Chiu, M. L.; Sligar, S. G.; Oldfield, E. *Biochemistry* **1991**, *30*, 2333−2347. (b) Lee, H. C.; Oldfield, E. *J. Am. Chem. Soc.* **1989**, *111*, 1584−1590.
(12) (a) McMahon, M. T.; deDios, A. C.; Godbout, N.; Saltzmann, R.; Laws, D. D.; Le, H.; Halvin, R. H.; Oldfield, E. *J. Am. Chem. Soc.* **1998**, *120*, 4784−4797. (b) Saltzmann, R.; Kaupp, M.; McMahon, M. T.; Oldfield, E. *J. Am. Chem. Soc.* **1998**, *120*, 4771−4783. (c) Halvin, R. H.; Godbout, N.; Saltzmann, R.; Wojdelski, M.; Arnold, W.; Schulz, C. E.; Oldfield, E. *J. Am. Chem. Soc.* **1998**, *120*, 3144−3151. (d) Saltzmann, R.; Ziegler, C. J.; Godbout, N.; McMahon, M. T.; Suslick, K. S.; Oldfield, E. *J. Am. Chem. Soc.* **1998**, *120*, 11323−11334. (e) Lee, H. C.; Cummings, K.; Hall, K.; Hager, L. P.; Oldfield, E. *J. Biol. Chem.* **1988**, *263*, 16118−16124.
(13) (a) Augspurger, J. D.; Dykstra, C. E.; Oldfield, E. *J. Am. Chem. Soc.* **1991**, *113*, 2447−2451. (b) Augspurger, J. D.; Dykstra, C. E.; Oldfield, E.; Pearson, J. G. In *Nuclear Magnetic Shieldings and Molecular Structure*; Tossell, J. A., Ed.; NATO ASI Series C386; Kluwer Academic Publishers: Dordrecht, The Netherlands, 1993; pp 75−94. (c) Augspurger, J. D.; Dykstra, C. E. *J. Phys. Chem.* **1991**, *95*, 9230−9234. (d) Augspurger, J. D.; Pearson, J. G.; Oldfield, E.; Dykstra, C. E.; Park, K. D.; Schwartz, D. *J. Magn. Reson.* **1992**, *100*, 342−357.
(14) de Dios, A. C.; Earle, E. M. *J. Phys. Chem. A* **1997**, *101*, 8132−8134.
(15) Kushkuley, B.; Stavrov, S. S. *Biophys. J.* **1997**, *72*, 899−912.
(16) Slebodnick, C.; Ibers, J. A. *J. Biol. Inorg. Chem.* **1997**, *2*, 521−525.
(17) Tetreau, C.; Lavalette, D.; Momenteau, M.; Fischer, J.; Weiss, R. *J. Am. Chem. Soc.* **1994**, *116*, 11840−11848.
(18) Slebodnick, C.; Fettinger, J. C.; Peterson, H. B.; Ibers, J. A. *J. Am. Chem. Soc.* **1996**, *118*, 3216−3224.
(19) Kim, K.; Fettinger, J.; Sessler, J. L.; Cyr, M.; Hugdahl, J.; Collman, J. P.; Ibers, J. A. *J. Am. Chem. Soc.* **1989**, *111*, 403−405.
(20) Kim, K.; Ibers, J. A. *J. Am. Chem. Soc.* **1991**, *113*, 6077−6081.

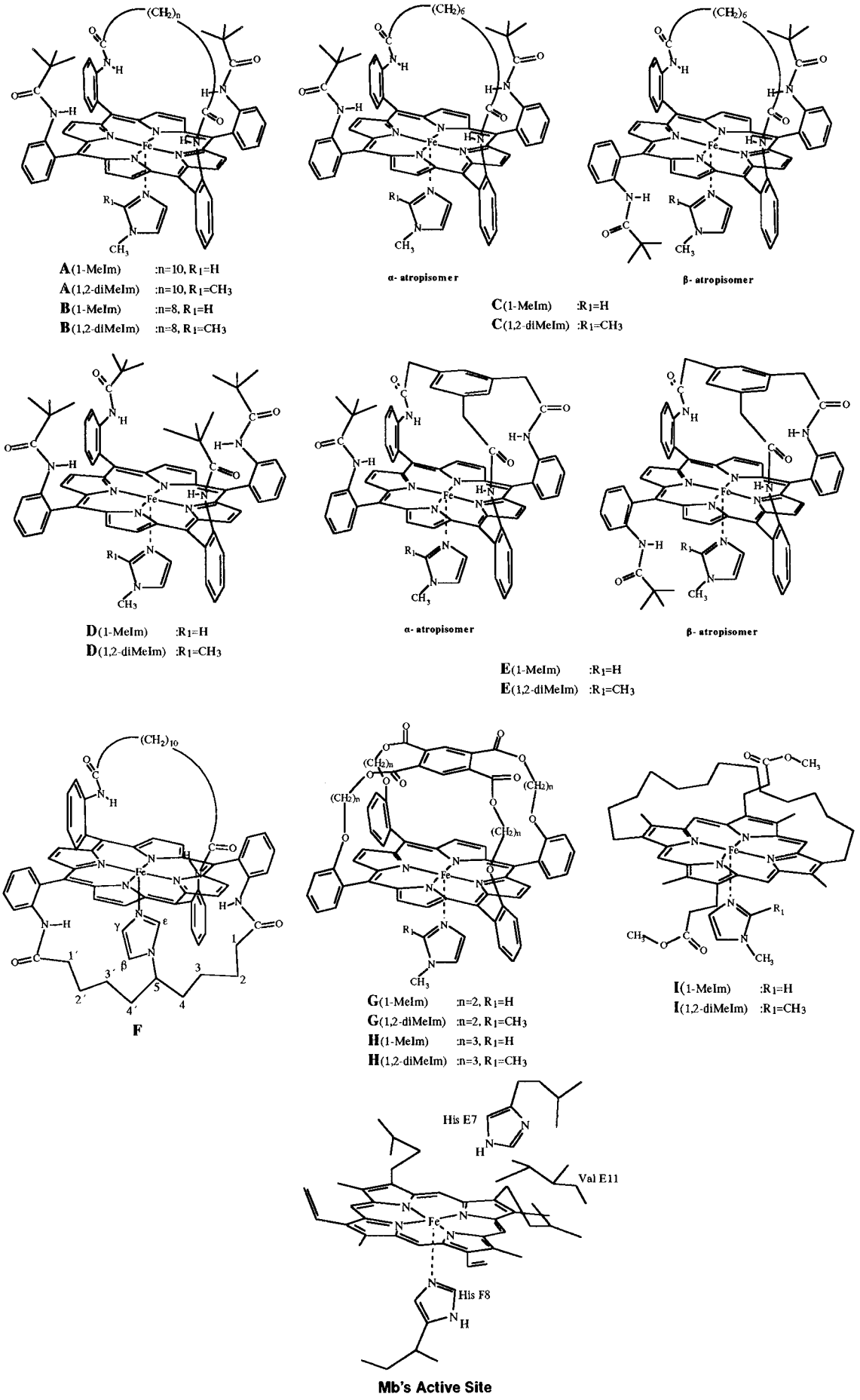

Figure 1. Schematic structures of the heme model compounds studied in this work; the active site of Mb is also included for comparison.

For experiments with carbon monoxide in a variety of deuterated solvents, gaseous carbon monoxide (99.7% enriched in ^{13}C, 0.9% in ^{17}O, and 11.9% in ^{18}O) was added to the solvents and the 5 mm NMR tubes were sealed under presure of ~1 atm.

NMR Spectra. ^{13}C NMR spectra were obtained at 100.62 and 150.90 MHz with Bruker AMX-400 and AVANCE 600 instruments, respectively, equipped with high-resolution probes (5 mm sample tubes). The chemical shifts were determined relative to the resonance position of the solvent (CD_2C1_2 ~53.8 ppm). Solvent suppression was achieved by selective irradiation. Overlapping resonances were resolution enhanced by multiplication of the free-induction decay with a Gaussian-exponential function. This function has the form $\exp(at - bt^2)$, where a (>0) and b (>0) are adjustable parameters. ^{17}O NMR spectra were obtained at 81.37 and 40.69 MHz with Bruker AVANCE 600 and 300 instruments, respectively, equipped with high-resolution multinuclear probes (5 mm sample tubes). The chemical shifts were determined relative to external H_2O or 1,4-dioxane (0.0 ppm).

Results and Discussion

^{13}C and ^{17}O Shieldings of Carbon Monoxide in Various Solvents. As a first step toward a detailed, quantitative model of distal ligand effects on carbonmonoxy hemoproteins Augspurger et al.[13] reported a theoretical correlation of $\delta(^{13}C)$, $\delta(^{17}O)$, and ^{17}O NQCCs with vibrational frequencies of isolated CO upon varying an external electrical perturbation by the use of the derivative Hartree−Fock (DHF) approach. External perturbing electrical potentials of three types were considered: a uniform electric field, a field gradient, and a potential due to a dipole oriented either along or perpendicular to the CO axis. For each type of environment $\delta(^{13}C)$ and $\delta(^{17}O)$ vary strongly with the vibrational $\nu(C-O)$ frequency shift, at least for frequency shifts of up to ± 50 cm^{-1}. Beyond that, there is a slight curvature. The linear relationship, which is opposite for ^{13}C and ^{17}O, is similar to that found for heme proteins. This led to the hypothesis that electrically perturbed carbon monoxide is a possible model for distal ligand effects in carbonmonoxy heme proteins. Furthermore, it was suggested that CO complexation to a metal is not likely to make a sharp change in the shielding polarizability.

The ^{13}C-labeled carbon monoxide from commercial sources normally has a considerable enrichment in ^{17}O and ^{18}O content, which makes it possible to obtain information on ^{13}C and ^{17}O shieldings and ^{18}O isotope shifts on ^{13}C of the same sample.[8b] Figure 2 shows typical ^{13}C NMR spectra of the ^{13}CO (99.7% enriched in ^{13}C, 0.9% in ^{17}O, and 11.9% in ^{18}O) in hexane and $CDCl_3$ solution. The asterisks denote the ^{18}O isotopically shifted ^{13}C resonances. Figure 3 shows a typical ^{17}O NMR spectrum of ^{13}CO in hexane and illustrates the advantages of working with ^{13}CO enriched to 0.9% in ^{17}O. Nevertheless, even with this level of enrichment no signal could be detected in H_2O or CF_3COOD solution with CO concentration less than 1 mM.

From Table 1 it is evident that oxygen-18 isotope effects on the ^{13}C shielding, $^1\Delta^{13}C(^{18/16}O)$, and ^{17}O shieldings, $\delta(^{17}O)$, are practically independent of the nature, dielectric constant and solvation ability of the solvent. The ^{13}C shieldings and $\nu(C-O)$ vibrational frequencies indicate a small variation. However, the ^{13}C resonance of the reference standard TMS has been shown to suffer solvents shifts up to ± 1.5 ppm in common NMR solvents at infinite dilution.[21] After bulk magnetic susceptibility correction it is evident that the ^{13}C shieldings of dissolved CO are practically independent of the solvation ability and dielectric constant of the solvent (Table 1).

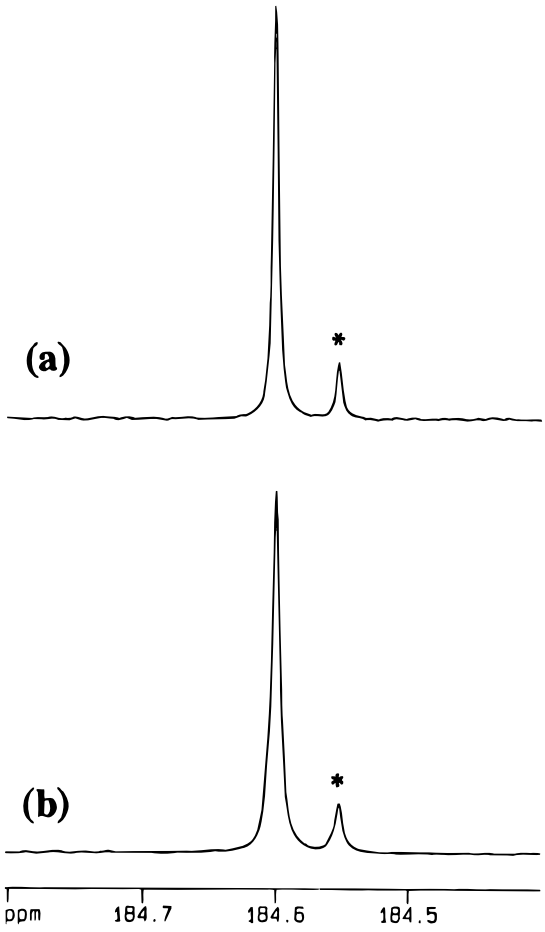

Figure 2. ^{13}C NMR spectra of ^{13}CO (99.7% enriched in ^{13}C, 0.9% in ^{17}O, and 11.9% in ^{18}O) in (a) H_2O and (b) $CDC1_3$ at 293 K using a Bruker AVANCE 600 instrument, T_{acq} ~ 0.8 s, 500 scans. The asterisks denote the ^{18}O isotopically shifted ^{13}C resonances.

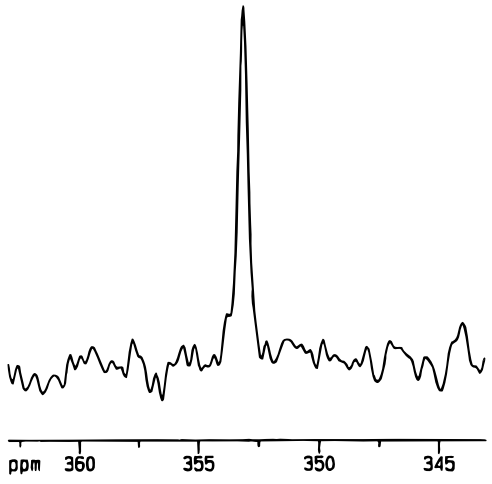

Figure 3. ^{17}O NMR spectra of ^{13}CO (99.7% enriched in ^{13}C, 0.9% in ^{17}O and 11.9% in ^{18}O) in hexane, at 293 K using a Bruker AVANCE 600 instrument, 90° pulse length ~8.3 μs, 500 000 scans, T_{acq} = 34 ms, preacquisition delay = 30 μs, exponential multiplication of the FID (LB = 20 Hz).

Table 2 shows representative literature dipole shielding polarizabilities $\bar{A}x$, dipole shielding hyperpolarizabilities $\bar{B}x$ and quadrupole shielding polarizabilities $\bar{C}xx$ for CO and H_2CO. For a range of fields of ~0.006 au (~3×10^7 V cm^{-1}), which is a reasonable value for a medium of low dielectric constant ($\epsilon \approx 2$), one would predict for $C^{17}O$ a dipole shielding polarizability term of ~1526.7 × 0.006 ≈ 9.2 ppm.[13] For $\bar{B}x$

(21) Ziessow, D.; Carrol, M. *Ber. Bunsenges. Phys. Chem.* **1972**, *76*, 61−64.

Table 1. ^{13}C Chemical Shifts, $\delta(^{13}C)$, ^{17}O Chemical Shifts, $\delta(^{17}O)$, and $^{16}O/^{18}O$ Isotope Shifts on ^{13}C Chemical Shifts, $^{1}\Delta^{13}C$ ($^{16}O/^{18}O$), of Carbon Monoxide Dissolved in Various Solvents of Dielectric Constant ϵ

solvent	ϵ	$\delta(^{13}C)^a$ (ppm)	$\delta(^{13}C)^b$ (ppm)	$\delta(^{13}C)^c$ (ppm)	$\delta(^{17}O)^d$ (ppm)	$^{1}\Delta^{13}C(^{16}O/^{18}O)$ (ppb)	ν(C−O) (cm^{-1})
hexane	2.0	184.9	184.7		352.9	49	
CCl_4	2.2	184.2	184.8	184.9	353.8	48	2135[e]
toluene	2.4	184.5	184.2	184.4	353.3	48	
$CDCl_3$	4.8	184.2	184.6	184.6	353.2	48	2138[e]
CD_2Cl_2	8.9	184.6	184.6	184.6	353.2	48	2136[e]
CD_3OD	32.7	185.5	184.2	184.9	352.4	49	
DMSO	46.7	184.2	185.1	185.3	354.2	49	
H_2O	78.5	186.9	184.6	184.6	353.2[f]	49	
CF_3COOD		188.0	185.0		—[g]	48	

[a] Relative to internal standard TMS in organic solvents or TSPSA in H_2O and CF_3COOD. [b] Constant field correction (with reference to CD_2C1_2). [c] Constant field correction and magnetic susceptibility correction. [d] External reference H_2O. [e] Baude, S.; Idrissi, A.; Turrell, G. *Can. J. Appl. Spectroscop.* **1996**, *41*, 60−64. [f] Reference 12e. [g] No resonance could be detected (see text).

Table 2. Representative Literature $\bar{A}x$, $\bar{B}x$, and $\bar{C}xx$ Shielding Polarizabilities

molecule	$\bar{A}x$ (ppm/au field)[a]	$\bar{B}x$ (ppm/au field^2)[b]	$\bar{C}xx$ (ppm/au efg)[c]
$\overline{C}O$[d]	374.5	535.5	−532.7
$\overline{H}_2\overline{C}O$[d]	697.4	3874.9	−746.0
$\overline{C}\overline{O}$[d]	1526.7	5906.1	1044.0
$\overline{H}_2\overline{C}\overline{O}$[d]	7018.9	70843.0	1377.8

[a] Dipole shielding polarizability $\bar{A}x$ in ppm/au field; 1 au field = 5.14225×10^9 V cm^{-1}. [b] Dipole shielding polarizability $\bar{B}x$ in ppm/au field^2. [c] Quadrupole shielding polarizability $\bar{C}xx$ in ppm/au electric field gradient; 1 au efg = 9.717447×10^7 V cm^{-2}. [d] Reference 13c,d.

= 5906.1 ppm/au, the shift is ~5906.1 × $(0.006)^2$ = 0.21 ppm. For $\bar{C}xx = 1044.0 \times 0.001 = 1.04$ ppm. For ^{13}CO the respective values are $\bar{A}x = 2.25$ ppm, $\bar{B}x = 0.02$ ppm, and $\bar{C}xx = 0.53$ ppm. These calculations clearly indicate that the dipole shielding polarizability makes a major contribution to both $\delta(^{17}O)$ and $\delta(^{13}C)$ even in media of low dielectric constant. This is in contrast with our experimental results which demonstrate that both $\delta(^{17}O)$ and $\delta(^{13}C)$ are practically independent of the dielectric constant and solvation ability of the medium.

Interestingly, the experimental data of the dependence of $\delta(^{17}O)$ of carbonyl compounds upon the dielectric constant of the medium indicate a very significant shielding of ~20 ppm in a medium of $\epsilon = 2$.[22] This shielding variation, which is approximately twice compared with that calculated from the dipole shielding polarizabilities of Table 2, should be attributed to the greater polarizability of the carbonyl oxygen compared with that of carbon monoxide.

^{13}C and ^{17}O Shieldings of the Fe−C−O Unit. A semiempirical explanation for the variation of the carbonyl ^{13}C and ^{17}O resonances in most transition-metal carbonyl complexes has been proposed by Buchner and Schenk.[23] These authors suggested that the dominant factor for the ^{13}C nuclei in the Karplus and Pople equation is the term

$$Q_{CC} + Q_{CO} + Q_{FeC} = \frac{4}{3}[1 - P^{\sigma}_{z_c z_o} P^{\pi}_{y_c y_o} - 3^{1/2} P^{\sigma}_{z_c z^2_{Fe}} P^{\pi}_{y_c yz_{Fe}}] \quad (1)$$

while for ^{17}O nuclei the term

$$Q_{OO} + Q_{CO} = \frac{4}{3}[1 - P^{\sigma}_{z_o z_c} P^{\pi}_{y_o y_c}] \quad (2)$$

where $P^{\pi}_{y_c yz_{Fe}}$ is the C−Fe(d_{yz}) π-bond order, $P^{\sigma}_{z_c z^2_{Fe}}$ is the C−Fe(d_{z^2}) σ-bond order, $P^{\sigma}_{z_c z_o}$ is the C−O σ-bond order, and $P^{\pi}_{y_c y_o}$ is the C−O π-bond order.

If there is relatively little π bonding between the metal and the carbonyl ligand, the decrease in the $-P^{\sigma}_{z_c z_o} P^{\pi}_{y_c y_o}$ term will be larger than the increase in the $-P^{\sigma}_{z_c z^2_{Fe}} P^{\pi}_{y_c yz_{Fe}}$ term, and there will be a ^{13}C shielding contribution in eq 1. In contrast, if there is significant π bonding between the metal and the carbonyl ligand, the increase will be larger than the decrease, and there will be a deshielding contribution in ^{13}C (eq 1). As noted by Buchner and Schenk,[23] as the σ-bond order of $P^{\sigma}_{z_c z_o}$ is negative, a reduction in the C−O π-bond order $P^{\pi}_{y_c y_o}$ results in a smaller value for $Q_{OO} + Q_{CO}$ in eq 2, i.e., the ^{17}O resonance is shielded upon back-bonding. This negative $\delta(^{13}C)$ vs $\delta(^{17}O)$ correlation has been reported for a variety of metal carbonyl complexes although an unusual positive correlation for a series of carbonyl (4-substituted pyridine) (*meso*-tetraphenylporphyrinato)Fe^{II} complexes has also been reported.[24]

The so-called "hybrid" models **A**−**C** have two pivalamido pickets (as in the "picket fence" porphyrin **D**) on each side of an amide handle of variable length linked in a cross-trans configuration (Figure 1, Table 3).[25] The X-ray structures of the hybrid complexes **A**(1-MeIm)[26] and **B**(1-MeIm)[17] show that the Fe−C−O unit is both linear and normal to the mean porphyrin plane. All contacts between the terminal oxygen atom and the aliphatic bridging chain are longer than 4 Å and the distance between the porphyrin mean plane and the aliphatic bridging chain is ≥8.4 Å (Table 4). For complex **C**(1-MeIm) the X-ray structural data show a very small bending of the Fe−C−O unit ($\theta = 178.3°$) without tilting.[17] Moreover, the iron atom lies almost in the plane formed by the porphyrin nitrogens but is slightly displaced from the 24-atom core mean plane toward the 1-MeIm ligand.

The hybrid models **A**−**C** have amide links, with four N−H dipoles in the heme pocket. The distance of the secondary amide

(22) Gerothanassis, I. P.; Vakka, C.; Troganis, A. *J. Magn. Reson. B* **1996**, *111*, 220−229.
(23) Buchner, W.; Schenk, W. A. *J. Magn. Reson.* **1982**, *48*, 148−151.
(24) Box, J. W.; Gray, G. M. *Inorg. Chem.* **1987**, *26*, 2774−2778.
(25) Abbreviations used: Hb, hemoglobin; Mb, myoglobin; TPP, tetraphenyl porphyrin; 1-MeIm, 1-methylimidazole; 1,2-diMeIm, 1,2-dimethylimidazole; **A**, α-5,15-[2,2′-(dodecanediamido)diphenyl]-α,α-10,20-bis(*o*-pivaloylamidophenyl)porphyrin; **B**, α-5,15-[2,2′-(decanediamido)-diphenyl]-α,α-10,20-bis(*o*-pivaloylamidophenyl)porphyrin; **C**, α-5,-15-[2,2′-(octane diamido)diphenyl]-α,α-10,20-bis(*o*-pivaloylamidophenyl)porphyrin; **D**, 5,10,15,20-(α,α,α,α)-(*o*-pivaloylamidophenyl)-porphyrin; **E**, 5,10,15-(1,3,5-benzene triacetyl)-tris(α,α, α-*o*-amidophenyl)-20-(α-*o*-pivaloylamidophenyl)porphyrin; **F**, α-5,15-[2,2′-(dodecanediamido)diphenyl]-*β*-10,20-{2,2′-(5-imidazol-1-ylnonane-1,9-diamido)diphenyl}porphyrin; **G**, 5,10,15,20-[pyrromellitoyltetrakis-*o*-oxyethoxyphenyl]porphyrin; **H**, 5,10,15,20-[pyrromellitoyltetrakis-*o*-oxypropoxyphenyl]porphyrin; **I**, 8,18-bis(methylpropoxyl)-3,7,13,17-tetramethyl-2,12-(tetradecamethylene)porphyrin. Schematic structures of the model porphyrins are shown in Figure 1.
(26) Ricard, L.; Weiss, R.; Momenteau, M. *J. Chem. Soc., Chem. Commun.* **1986**, 818−820.

Table 3. ^{13}C Chemical Shifts, $\delta(^{13}C)$, ^{17}O Chemical Shifts, $\delta(^{17}O)$, $^{16}O/^{18}O$ Isotope Shifts on ^{13}C Shieldings, $^1\Delta(^{16}O/^{18}O)$, and C−O Vibrational Frequencies, ν(C−O), of the Heme Model Compounds of Figure 1 and Selected Heme Proteins

no.[a]	compound	$\delta(^{13}C)$ (ppm)	$\delta(^{17}O)$ (ppm)	$^1\Delta(^{16}O/^{18}O)$ (ppb)	ν(C−O) (cm^{-1})
1	Fe(TPP(1-MeIm)	205.0	372.0		1969[b]
2	Fe a(BHP)(C_9-Im)(C_{12})[c]	203.9 204.4	374.6	29.7 28.9	1971[d]
3	Fe(TPivP)(1-MeIm)	204.7	375.2	29.0	1969[e]
4	Fe(TPivP)(1,2-diMeIm)	205.0	379.0	27.0	1962[e]
5	Fe(PocPiv)(1-MeIm)	204.6		28.0	1964 [f]
6	α-Fe(PocPiv)(1,2-diMeIm) [g]	204.7	366.1	26.6	
7	β-Fe(PocPiv)(1,2-diMeIm) [h]	204.6	369.2	27.6	
8	Fe(C_2-Cap)(1-MeIm)	202.1	371.0	32.0	2002[i]
9	Fe(C_2-Cap)(1,2-diMeIm)	202.2	375.9		1999[i]
10	Fe(C_3-Cap)(1-MeIm)	203.0	375.0	32.5	1979[i]
11	Fe(C_3-Cap)(1,2-diMeIm)	203.1	377.0		1984[i]
12	Fe(PLC14)(1-MeIm)	204.9	369.6	27.5	
13	Fe(PLC14)(1,2-diMeIm)	205.4	370.5		
14	α-Fe(Piv_2C_8)(1-MeIm) [g]	206.0	362.1	26.0	1948[d]
15	β-Fe(Piv_2C_8)(1-MeIm) [h]	205.8	367.9	26.0	
16	α-Fe(Piv_2C_8)(1,2-diMeIm) [g]	206.2	362.3	27.7	
17	β-Fe(Piv_2C_8)(1,2-diMeIm) [h]	206.0	369.0	26.2	
18	Fe(Piv_2C_{10})(1-MeIm)	205.3	367.0	26.5	1952[d]
19	Fe(Piv_2C_{10})(1,2-diMeIm)	205.6	368.4	28.0	
20	Fe(Piv_2C_{12})(1-MeIm)	205.0	370.7	27.0	1958[d]
21	Fe(Piv_2C_{12})(1,2-diMeIm)	205.6	372.8	27.0	
22	horseradish peroxidase isoenzyme C, pH = 7		358.4 [j]		1913[k]
23	pH = 6.4	209.1[l]	358.0 [j]		1913[k]
24	pH = 10.5		365.0 [j]		1932[k]
25	horseradish peroxidase isoenzyme A, pH = 4.5		355.5 [j]		1909[k]
26	pH = 6.8	208.9 [l]	361.0 [j]		1923[k]
27	pH = 9.5		362.6 [j]		1932[k]
28	chloroperoxidase		368.6 [j]		1958[m]
29	rabbit Hb, α chain	208.0[n]	361.4 [j]		1928[o]
30	rabbit Hb, β chain	206.4[n]	369.5 [j]		1951[o]
31	human Hb, α chain	206.4[n]	369.0 [j]		1951[p]
32	human Hb, β chain	206.2[n]	369.0 [j]		1951[p]
33	sperm whale Mb, pH = "low"		370.7 [j]		1967[q]
34	sperm whale Mb, pH = 7	207.9 [r]	366.5 [j]		1944[r]
35	sperm whale Mb (HisE7 Phe)		371.7 [j]		1967[j]
36	sperm whale Mb(HisE7 Val)		371.7 [j]		1970[j]
37	sperm whale Mb A_0	205.5 [j]	372.0 [j]		1969[j]
38	sperm whale Mb A_1	207.2 [j]	366.0 [j]		1944[j]
39	*G. dibranchiata* Hb	205.9 [j]	372.7 [j]		1970[j]

[a] Numbered entries are plotted in Figures 5, 6, and 7. [b] Reference 12a. [c] Two different conformers (see text). [d] Reference 30. [e] Reference 31. [f] Reference 4b. [g] α denotes α-atropisomer (see text). [h] β denotes β-atropisomer (see text). [i] Reference 32. [j] Reference 11a. [k] Reference 33. [l] Reference 34. [m] Reference 35. [n] Reference 36. [o] Reference 37. [p] Reference 38. [q] Reference 39. [r] Reference 40.

groups of the chain and the CO ligand, N(H)···O(C), is 4.60 Å for model **A**, thus providing an environment of positive polarity for the CO ligand. This polar interaction can be increased via the steric constraint of a short strap. Thus increase in the polar interaction might be expected for the **C**(1-MeIm) model, with an N(H) (amide)···O(C) distance of 3.99 Å, compared to that of the model **A**(1-MeIm) and the picket fence model **D** with an N(H) (amide)···O(C) distance of 4.90 Å. This distal polar and electric field effect can be schematically pictured by considering the resonant structures of the FeCO group (Scheme 1).

Scheme 1

$$\underset{\textbf{(a)}}{Fe^{-}-C\equiv O^{+}} + {}^{\delta+}H \leftrightarrow \underset{\textbf{(b)}}{Fe=C=O^{\delta+}-H} \leftrightarrow \underset{\textbf{(c)}}{Fe=C=O} + {}^{\delta+}H$$

A positive potential near the CO carbon atom, as would be the case of the NH dipoles of the amide links, will favor resonance **1(c)** (decrease in the C−O π-bond order and an increase in the Fe−C π-bond order). As discussed before, if there is significant increase in π bonding between the metal and the carbonyl ligand there will be a deshielding contribution in ^{13}C and a shielding contribution in ^{17}O. This is in agreement with the experimental data of Table 3 which show a progressive increase of $\delta(^{13}C)$ and decrease of $\delta(^{17}O)$ upon handle shortening in the hybrid models. The ^{13}C and ^{17}O NMR spectra of the hybrid model **C**(1-MeIm) and **C**(1,2-diMeIm) (Figure 4d) indicate the presence of two resonances which can be attributed to α- and β-atropisomerization of one of the untethered picket which occured during the iron(II) insertion into the free base (this entailed the heating of the solution to 80 °C). Although the ^{13}C shielding differences are only 0.2 ppm for both the 1-MeIm and 1,2-diMeIm complexes, the ^{17}O shielding differences are 7.8 and 6.7 ppm, respectively (Figure 4d). Since the NH(amide)···O(CO) distances of the untethered pickets (5.10 and 5.40 Å) are significantly longer compared with that of the handle (3.99 and 4.19 Å), it can be concluded that $\delta(^{17}O)$ is not primarily influenced by the local distal field interactions.

The ^{13}C NMR spectra of the ^{13}CO complex of the Fe^{II}PocPiv-(1,2-diMeIm) model, **E**(1,2-diMeIm), indicates the presence of two strongly overlapped resonances which are better resolved

Table 4. Structural Features and Rates of CO Desorption, k^{-CO}, for CO Binding with the Heme Model Compounds of Figure 1

compound	C−O bond length (Å)	Fe−C bond length (Å)	Fe−M distance[a] (Å)	N(H) (amide)···O(C) distance (Å)	Fe−C−O angle (°)	$10^3\,k^{-CO}$ (s^{-1})
A(1-MeIm)	1.149(6)	1.728(6)	8.43	4.60, 4.90	180.0	2.7
A(1,2-diMeIm)						110
B(1-MeIm)	1.149(6)	1.752(4)	6.81	4.42, 4.72, 5.10, 5.30	178.9	2.0
B(1,2-diMeIm)						50
C(1-MeIm)	1.149(6)	1.733(4)	6.53	3.99, 4.19, 5.10, 5.40	178.3	8.2
C(1,2-diMeIm)						80
D(1-MeIm)				4.90[d]		7.8
D(1,2-diMeIm)						140
E(1-MeIm)						8.6
E(1,2-diMeIm)[b]	1.148(7)	1.768(7)	5.36	3.76, 6.33, 4.55	172.5	55.0
F				4.60[e]		6.7
G(1-MeIm)[c]	1.161(8)	1.742(7)	5.57		172.9	50
	1.159(8)	1.748(7)	5.68		175.9	
G(1,2-diMeIm)						
H(1-MeIm)	1.107(13)	1.800(13)	5.86		178.0	
H(1,2-diMeIm)						
I(1-MeIm)						110
I(1,2-diMeIm)						560

[a] Fe−M is the distance between the centroid of distal cap or strap and the Fe atom; it defines the distal pocket size. [b] β-Atropisomer. [c] These are two independent Fe(C_2-Cap)(1-MeIm)(CO) molecules within the asymmetric part of the unit cell. [d] Estimated from the analogous untethered-picket distances in the crystal structure of **A**(1-MeIm)(CO). [e] Estimated from the analogous tethered-picket distances in the crystal structure of **A**(1-MeIm)(CO).

at lower temperatures (290 K).[10a] The two signals, with relative integrals 3:2, can be attributed to α- and β-atropisomerization of the fourth untethered picket which occurred during the iron(II) insertion into the free-base. Assignment of the two atropisomers was based on the NOE effect between the protons of the methyl groups of the "β-picket" and the -N(CH_3) protons of the axial imidazole. The ^{17}O NMR spectrum indicates the presence of two distinct resonances with a chemical shift difference of 3.1 ppm (Figure 4c). This provides direct evidence that significant electronic changes occur at the oxygen atom of the two atropisomers. Kim et al.[19] have reported the X-ray crystal structure of the β-atropisomer of **E**(1,2-diMeIm) (in which the fourth picket group is in the "down" position). The Fe−C−O bond angle was found to be 172.5° (Table 4). The modest distortion of the Fe−C−O unit is accompanied by considerable ruffling of the porphyrin periphery and significant shifting of the benzene "cap" away from the bound CO ligand. The crystal structure shows that the distance between the O atom of the bound CO and the three inequivalent amide N atoms is 3.76, 4.55, and 6.33 Å versus 3.99 and 4.19 Å for the two amide NH groups of the handle and 5.10 and 5.40 Å for the two picket NH groups for the **C**(1-MeIm) model. This might result in a stronger NH (amide)···OC dipolar interaction in **C**(1-MeIm) compared with that in the **E**(1,2-diMeIm) model. As expected, the value of δ(^{13}C) of the bound CO in **E**(1,2-diMeIm) is 1.4 ppm lower than in **C**(1-MeIm) while δ(^{17}O) is 4.0 ppm higher. A complication, however, might result from the close contact of the carbonyl oxygen with the π electron cloud of the benzene ring. The distance between the carbonyl O atom and the center of the benzene cap is 3.99 Å and this might inhibit back-bonding in the FeCO unit (see discussion below).

The ^{13}C NMR spectrum of the so-called "hanging imidazole" model **F**, which has two NH dipoles turned toward the Fe−C−O unit, indicates the existence of two distinct resonances of ^{13}CO bound to iron with differences between the two magnetic environments (δ = 203.9 and 204.4 ppm, Table 3). These resonances, with relative population ~2:1, may be attributed to two forms of the model compound with two orientations of the axial imidazole which differ from each other by 180° as demonstrated by the use of 2D ^{1}H−^{1}H ROESY experiments. The major conformer indicates a strong ROE peak between the β proton of the hanging imidazole and the C_5 proton (H_5) of the strap; the minor conformer indicates an ROE peak between the ϵ proton of the imidazole and the H_5 proton of the strap. Evidently, the two environments are not identical since the two complexes are not related by the true symmetry axis. Therefore, changes in the orientation of axial ligand are capable of inducing differences in the ^{13}CO environment with possible consequences in the kinetics and thermodynamics of the CO binding to heme model compounds and proteins. Interestingly, La Mar and coworkers[27] have similary shown that the heme ring in myoglobin exist in two orientations differing by a 180° rotation about the α,γ-meso axis. The ^{17}O NMR spectrum indicates the presence of two strongly overlapped resonances. Simulation of the spectrum by Lorentzian lines could be performed. The chemical shifts were evaluated as δ = 374.8 ppm ($\Delta\nu_{1/2}$ = 80 Hz) and δ = 374.5 ppm ($\Delta\nu_{1/2}$ = 80 Hz) for the two forms, respectively. For the model **F** no X-ray structure is available. Molecular models indicate that the distance of the secondary amide groups of the chain and the CO ligand is ~4.60 Å, very similar to that for model **A**(1-MeIm).

For the **G**(1-MeIm) complex, in which a benzene cap is attached by carboxylate links and a pair of methylene groups to the four hydroxyl groups of tetrakis(*o*-hydroxylphenyl)-porphyrin, the refined X-ray crystal structure shows the presence of two crystallographically independent porphyrin molecules.[20] The Fe−C−O groups are distorted from linearity (172.9° and 175.9°, Table 4) and tilted off the axis normal to the porphyrin (off-axis displacement for the carbon atoms being 0.17 and 0.12 Å, respectively). These distortions result from short non-bonding interactions between the cap and the CO ligand. The cap is no longer parallel to the porphyrin plane and the porphyrin distortion is very small, presumably because of the constraint of the cap. Only a single ^{13}C and ^{17}O isotropic resonance is observed for **G**(1-MeIm). The very significant shielding of the ^{13}C resonance (δ = 202.1 ppm) compared to the other heme models probably results from the nature of the linkages from the porphyrin to the benzene cap. In C_2-Cap the lone pairs of the oxygen of the ester groups provide negative polarity.

(27) La Mar, G. N.; Pande, U.; Hauksson, J. B.; Pandey, B. K.; Smith, K. M. *J. Am. Chem. Soc.* **1989**, *111*, 485−491.

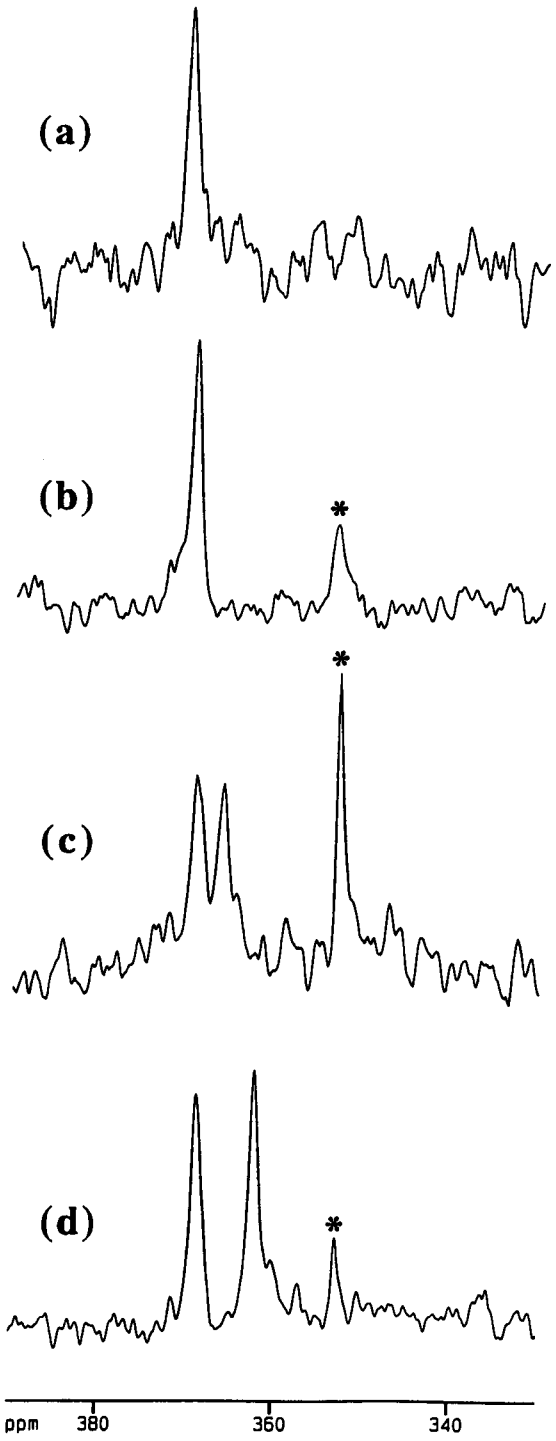

Figure 4. ^{17}O NMR spectra of the ^{13}CO complexes (99.7% enriched in ^{13}C, 0.9% in ^{17}O, and 11.9% in ^{18}O) of the heme models: (a) **A**(1-MeIm); (b) **I**(1-MeIm); (c) **E**(1,2-diMeIm); (d) **C**(1,2-diMeIm), saturated solution in CD_2Cl_2, at 293 K using a Bruker AVANCE 600 instrument, $T_{acq} \sim 33$ ms, preacquisition delay = 30 μs, 6×10^4, 12×10^4, 5×10^5, and 12×10^4 scans for (a), (b), (c), and (d), respectively, exponential multiplication of the FIDs (LB = 50 Hz). The asterisks denote the resonance absorption of free CO in solution.

Therefore, one would expect an increase in the π-bond order and thus decrease in $\delta(^{13}C)$.[8b,c] Furthermore, the π electron cloud of the benzene ring is expected to inhibit back-donation from the Fe(II) d_π to the CO π^* orbital. On the contrary, the ^{17}O shielding indicates a value which is very similar to that of the hybrid model **A**(1-MeIm) with four N−H dipoles turned toward the iron. This anomalous ^{17}O shielding cannot be attributed to the ring current of the aromatic cap; for a distance of ~2.77 and 2.80 Å between the center of the benzene ring and the CO oxygen for the two independent molecules in the cell, the expected ring current shift is only ~0.6 ppm.

For the **H**(1-MeIm) complex, in which the linker arms are extended by one methylene group, the shielding decreases (δ = 203.0 ppm) owing to attenuation of the benzene cap interaction. This provides further evidence in support of the hypothesis that $\delta(^{13}C)$ depend upon the π-bonding between the metal and the carbonyl ligand. Interestingly, the X-ray structure of Fe(C_3-Cap)(1-MeIm)(CO) indicates an untwisting of the cap which, in combination with the reorientation of the arms, causes a vertical expansion of the cap by 2.36 Å (~5.86 Å above the mean porphyrin plane) to accomodate CO, from 3.5 Å in H_2(C_3-Cap).[18] On the contrary, $\delta(^{17}O)$ indicates deshielding compared with that of complex **G**(1-MeIm) ($\delta(^{17}O)$ = 375.0 ppm, Table 3). This implies that $\delta(^{17}O)$ is not primarily influenced by the modulation of π back-bonding by the distal pocket polar interactions, although oxygen is the terminal atom of the Fe−CO unit and, thus, more susceptible to local interactions within the heme pocket.

For the "strapped" model **I**, no X-ray structure is available. This complex has significantly higher rate of CO desorption, k^{-CO}, than the other model compounds in this study (Table 4) which results in extensive broadening of both Fe−^{13}CO and ^{13}CO resonances at room temperature. The most likely reason for this high dissociation rate would be an increased bending of the Fe−C−O unit due to strong central steric interactions with the distal protecting chain. Both $\delta(^{13}C)$ and $\delta(^{17}O)$ are consistent with a significant degree in back-bonding despite the absence of a distal amide group. As discussed by Li and Spiro, FeCO bending should strongly decrease back-bonding.[4a] The electronic effect of FeCO tilting and porphyrin ruffling are more difficult to predict, but an increase in back-bonding is not an obvious result. As discussed in detail by Ray et al.[4b] back-bonding is also influenced by variations in the electron-donating tendency of the substituents of the porphyrin ring. Thus complexes based on substituted tetraaryl porphyrins are generally found lower on the back-bonding correlation than adducts based on C_β-alkyl-substituted porphyrins. The alkyl substituents are electron donating and enhance back-donation, while the phenyl substituents are electron withdrawing and decrease back-donation.

^{18}O Isotope Effects on ^{13}C Nuclear Shielding of CO in Various Solvents and the Fe−C−O Unit in Hemoprotein Models. It has been shown that one-bond isotope shifts of nucleus A due to substitution of ^{m}X by $^{m'}$X in a symmetrical AX molecule in which the mean bond angle distortions do not contribute significantly to the isotope shift, can be expressed as

$$^1\Delta A(^{m'/m}X) \approx (\partial\sigma^A/\partial\Delta r_{AX})_e \langle\Delta r\rangle \frac{m' - m}{m'} \frac{1}{2} \frac{m_A}{m_A + m} \quad (3)$$

where $\langle\Delta r\rangle$ is the mean bond displacement.[28] The electronic factor $(\partial\sigma^A/\partial\Delta r_{AX})_e$ reflects the range of chemical shifts for a given nucleus and depends largely on the paramagnetic term of nuclear shielding. Therefore, it is generally smaller for the more shielded nucleus. For a given nucleus A, $(\partial\sigma^A/\partial\Delta r_{AX})_e$ depends on the AX bond properties. In general its magnitude is greater for the stronger bond. Thus, it is expected to correlate with bond order and bond length.

(28) Jameson, C. J.; Osten, H.-J. *J. Am. Chem. Soc.* **1985**, *107*, 4158−4161.

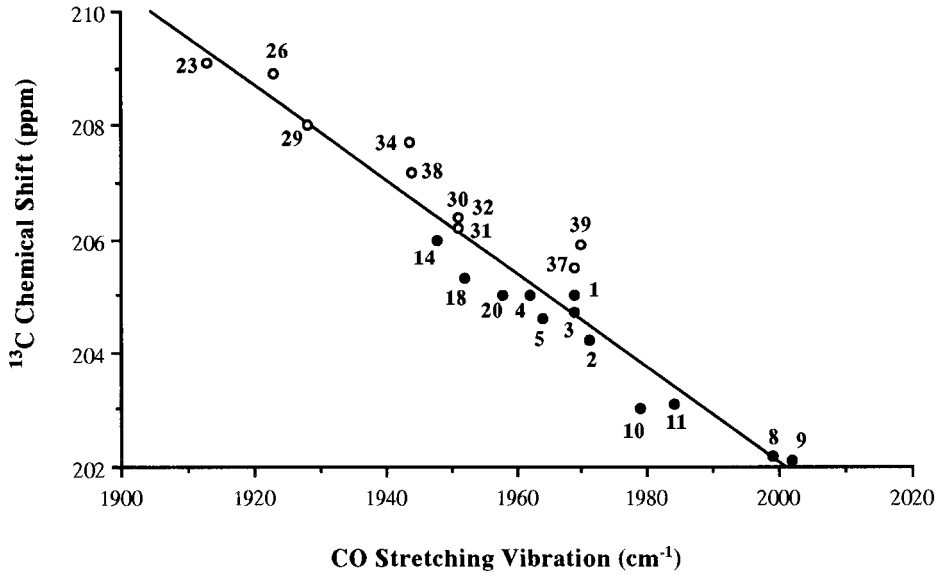

Figure 5. Plot showing relation between ^{13}C NMR isotropic chemical shift [δ(^{13}C), ppm] and infrared CO vibrational stretching frequency [ν(C−O), cm^{-1}] for heme model compounds (●) and a variety of hemoproteins (○). The numbers correspond to the entries in Table 3.

As expected upon substitution with the heavier isotope (^{18}O) the ^{13}C NMR signal shifts towards lower frequencies (higher shielding) (Figure 2). The ^{18}O isotope effects on the ^{13}C shielding of carbon monoxide are independent of the nature, solvation ability and dielectric constant of the solvent (48−49 ppb, Table 1). The ^{18}O isotope effects on the ^{13}C shielding of the complexes **A**, **B**, and **C** are very similar, 2.6−2.7 Hz (26−27 ppb), and are smaller compared to the values (∼38 ppb) measured in a series of metal carbonyls.[29] The X-ray structures of the complexes **A**, **B**, and **C** show identical, within experimental error, C−O bond lengths (Table 4).[17,25] From the direct comparison of $^{1}\Delta^{13}$C($^{18/16}$O) of compounds **A**, **B**, and **C** with $^{1}\Delta^{13}$C($^{18/16}$O) of CO itself, it can be concluded that the CO bond length in heme models is significantly reduced compared with the free CO, in agreement with the structural data of Table 4. The C−O bond length of the Fe(C_3-Cap)(1-MeIm)(CO) model is shorter (∼1.107 Å) compared to other model compounds of Table 4 (average distance ∼1.150 Å) while that of the Fe(C_2-Cap)(1-MeIm)(CO) is longer (1.161 and 1.158 Å). On the contrary, the isotope shifts of both complexes are very similar and larger compared with most of the model compounds of Figure 1. Thus it appears that the lack of correlation between $^{1}\Delta^{13}$C($^{18/16}$O) and crystallographic CO bond lengths reflects significant uncertainties in the X-ray determination of the carbon and oxygen position (esd's ≫ ∼0.01 Å).[4b]

Correlations between δ(^{13}C), δ(^{17}O), $^{1}\Delta^{13}$C($^{18/16}$O), and ν(C−O): Comparison with Hemoproteins. Several workers have noted a negative correlation between δ(^{13}C) vs ν(C−O) and δ(^{17}O) vs ν(C−O) for a variety of metal carbonyl adducts and have discussed this effect in terms of back-bonding in the FeCO unit.[7,8,11] When δ(^{13}C) is plotted against ν(C−O) for the CO adducts of the superstructured heme model compounds of Figure 1 and several hemoproteins (Table 3), an excellent linear correlation is then observed which can be expressed as

$$\delta(^{13}\text{C, ppm}) = -0.083\nu(\text{C−O, cm}^{-1}) + 368.0$$

with a correlation coefficient of 0.940 (Figure 5). The use of weighted-average ν(C−O) is required since hemoprotein subunits exhibit absorbance at more than one frequency due to multiple conformational substates whose rate of interconversion is greater than the NMR time scale (∼10^{-4} s).[7] The ^{13}C resonances of heme proteins cover a 3.5 ppm range and the computed weighted-average vibrational frequencies vary by 45 cm^{-1}. This range is extended to 7.0 ppm when the ^{13}C shieldings of the heme models are included. This demonstrates that both heme models and heme proteins are homogenous from the structural and electronic view point.[8b,c]

From the above it is evident that strong back-bonding, due to positive polar interactions within the heme pocket, decreases the C−O π-bond order and increases the deshielding for ^{13}C while simultaneously decreasing the ν(C−O). Interestingly, similar effects have been observed due to polar interactions with the solvent molecules. Thus the ^{13}C shieldings and ν(C−O) stretching frequencies of *N*-butylimidazole heme B dimethyl ester are sensitive to solvent parameters.[7] As solvent polarity increases, δ(^{13}C) indicates a progressive deshielding ($CC1_4$, 203.6 ppm; $CHC1_3$, 204.4 ppm; DMSO, 205.2 ppm) while ν(C−O) indicates a significant decrease ($CC1_4$, 1980 cm^{-1}; $CHC1_3$, 1968 cm^{-1}; DMSO, 1952 cm^{-1}).

According to this back-bonding model, one would predict a monotonic relation between $^{1}\Delta^{13}$C($^{18/16}$O), which is a monitor of the C−O bond length, and both δ(^{13}C) and ν(C−O).[8b] $^{1}\Delta^{13}$C($^{18/16}$O) shows a linear relationship as a function of δ(^{13}C), the actual values used being shown in Table 3, which can be

(29) Darensbourg, D. J.; Baldwin, B. J. *J. Am. Chem. Soc.* **1979**, *101*, 6447−6449.
(30) Desbois, A.; Momenteau, M.; Lutz, M. *Inorg. Chem.* **1989**, *28*, 825−835.
(31) Collman, J. P.; Brauman, J. I.; Halbert, T. R.; Suslick, K. S. *Proc. Natl. Acad. Sci. U.S.A.* **1976**, *73*, 3333−3337.
(32) Hashimoto, T.; Dyer, R. L.; Crossley, M. J.; Baldwin, J. E.; Basolo, F. *J. Am. Chem. Soc.* ***1982***, *104*, 2101−2109.
(33) Evangelista-Kirkup, R.; Smulevich, G.; Spiro, T. G. *Biochemistry* **1986**, *25*, 4420−4425.
(34) Behere, D. V.; Gonzalev-Vergara, E.; Goff, H. M. *Biochem. Biophys. Res. Commun.* **1985**, *131*, 607−613.
(35) O'Keefe, D. H.; Ebel, R. E.; Peterson, J. A.; Maxwell, J. C.; Caughey, W. S. *Biochemistry* **1978**, *17*, 5845−5852.
(36) Moon, R. B.; Richards, J. H. *Biochemistry* **1974**, *13*, 3437−3443.
(37) Satterlee, J. D.; Teintze, M.; Richards, J. H. *Biochemistry* **1978**, *17*, 1456−1462.
(38) Choc, M. G.; Caughey, W. S. *J. Biol. Chem.* **1981**, *256*, 1831.
(39) Ramsden, J.; Spiro, T. G. *Biochemistry* **1989**, *28*, 3125−3128.
(40) Perkins, T.; Satterlee, J. D.; Richards, J. H. *J. Am. Chem. Soc.* **1983**, *105*, 1350−1354.

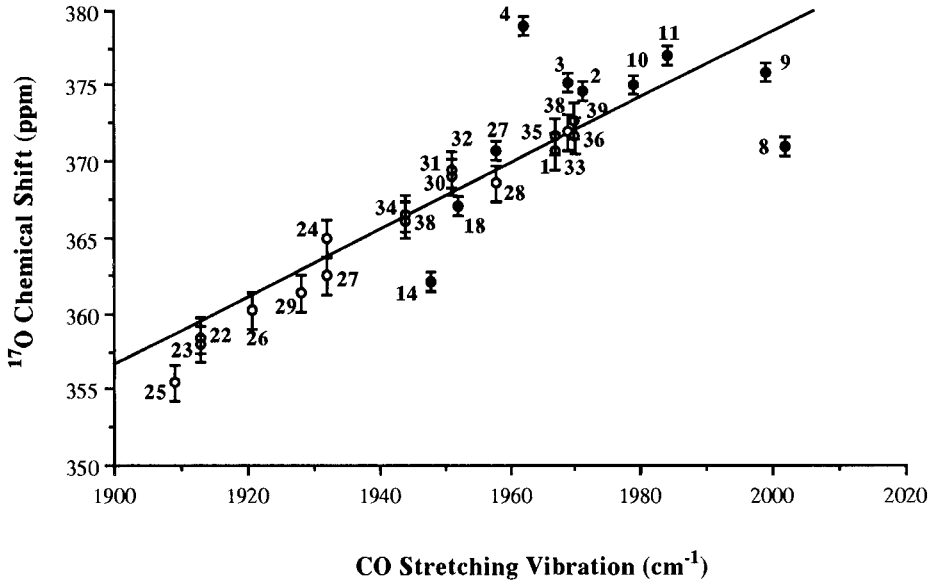

Figure 6. Plot showing relation between $\delta(^{17}O, ppm)$ and $\nu(C-O, cm^{-1})$ for heme model compounds (●) and a variety of hemoproteins (○). The numbers correspond to the entries in Table 3.

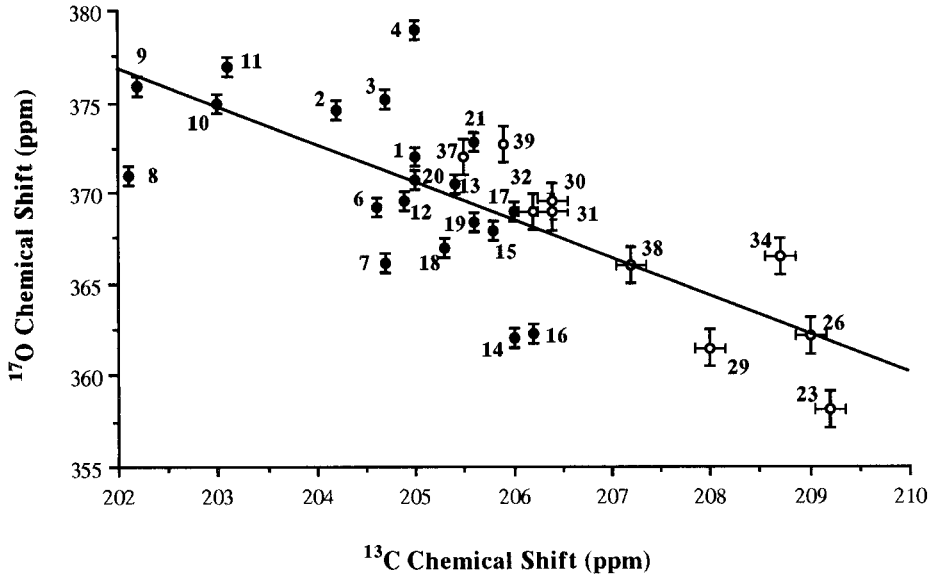

Figure 7. Plot showing relation between ^{17}O isotropic NMR chemical shifts [$\delta(^{17}O)$, ppm] and ^{13}C isotropic NMR chemical shifts [$\delta(^{13}C)$, ppm] for heme model compounds (●) and a variety of hemoproteins (○). The numbers correspond to the entries in Table 3.

expressed as

$$^{1}\Delta^{13}C(^{18/16}O, ppb) = -1.8918\ \delta(^{13}C, ppm) + 415.1$$

with a correlation coefficient of 0.874.

When the oxygen-17 chemical shifts, $\delta(^{17}O, ppm)$, for the heme model compounds of Figure 1 and a variety of hemoproteins are plotted against infrared CO vibrational stretching frequencies, $\nu(CO, cm^{-1})$, then paradoxically, a poor correlation is observed (Figure 6). The relationship can be expressed as

$$\delta(^{17}O, ppm) = 0.219\nu(C-O, cm^{-1}) - 59.52$$

with a correlation coefficient of 0.750. It should be noted that the data of heme proteins fall closer to the solid line.

A plot of $\delta(^{13}C)$ vs $\delta(^{17}O)$ for the heme model compounds of Figure 1 indicates the lack of correlation (correlation coefficient of 0.350) which is rather unusual since reasonable negative correlations have been reported for a variety of metal carbonyl complexes.[24] Inclusion of ^{17}O NMR data of several heme proteins indicates a very poor correlation which can be expressed as

$$\delta(^{17}O, ppm) = -2.093\delta(^{13}C, ppm) + 799.7$$

with a correlation coefficient of 0.582 (Figure 7). The ratio $\delta_i(^{17}O)/\delta_i(^{13}C) = 3.4$ is larger than the ratio ~2 reported for simple metal carbonyls[24] and smaller than the ratio 4.3 reported for hemoproteins.[11a]

The crystallographic distance between the center of the benzene ring and the CO oxygen is 3.99 Å for **E**(1,2-diMeIm), and 2.77 and 2.80 Å for the two independent molecules in the cell for **G**(1-MeIm) and 2.95 Å for **H**(1-MeIm). Therefore, the expected benzene ring current shielding of the CO oxygen should be 0.3, 0.7, and 0.6 ppm for **E**(1,2-diMeIm), **G**(1-MeIm), and **H**(1-MeIm), respectively. Correction of $\delta(^{17}O)$ for the benzene ring current shifts results only in marginal improvement of the correlation of $\delta(^{17}O)$ vs $\delta(^{13}C)$ (correlation coefficient ~ 0.590). It can be concluded that the lack of correlation

between $\delta(^{17}O)$ and $\delta(^{13}C)$ cannot be attributed to the ring current effect of the aromatic cap.

The oxygen-17 shielding differences of the two atropisomers of **E**(1,2-diMeIm), **C**(1-MeIm), and **C**(1,2-diMeIm) were found to be 3.1, 7.8, and 6.7 ppm, respectively. This provides direct evidence that very significant electronic changes occur at the oxygen atom of the CO ligand. Since the NH (amide)···O(CO) distance of the untethered picket (>5.10 Å) is significantly longer compared with those of the handle (3.99 Å) it can be concluded that the electronic difference between the two atropisomers cannot be attributed to differences in polar interactions with the NH groups of the organic superstructure. This implies that oxygen-17 shieldings are not primarily influenced by the local distal field interactions. This result appears surprising since oxygen is the terminal atom of the Fe−CO unit and, therefore, is more susceptible to local interactions within the heme pocket. Furthermore, the computed shielding polarizabilities of oxygen are significantly larger compared to those of carbon (Table 2). Recenly, it has been demonstrated that atropisomerism has a very significant effect on the degree of porphyrin ruffling with a profound effect on both the average shieldings of the meso carbons of the porphyrin skeleton[8a] and the iron-57 shieldings.[10a] It can, therefore, be concluded that porphyrin ruffling has a significant effect on $\delta(^{17}O)$, contrary to recent theoretical calculations[15] which indicated that heme distortions have a minor effect on ^{17}O isotropic shifts.

Conclusions

The ^{13}C shieldings of several carbonmonoxide heme models, with varying polar and steric effects of the distal organic superstructure and constraints of the proximal side, and of several HbCO and MbCO species at different pH values cover a 7.0 ppm range. The excellent linear $\delta(^{13}C)$ vs $\nu(C-O)$ relationship proves that both IR and NMR measurements reflect a similar type of electronic interaction. Positive polar interactions of bound CO with distal residues decrease the C−O π-bond order resulting in an increase in $\delta(^{13}C)$ and decrease in $\nu(C-O)$. Negative polar interactions reverse the above effects. $\nu(C-O)$, $\delta(^{13}C)$, and $^1\Delta^{13}C(^{18/16}O)$ parameters of heme model compounds reflect similar interaction which is primarily the modulation of π back-bonding from Fe d_π to CO π^* orbital by the distal pocket polar interactions. $\delta(^{13}C)$, $\delta(^{17}O)$, and $^1\Delta^{13}C(^{18/16}O)$ of carbon monoxide are practically independent of the solvation ability and dielectric constant of the medium. This suggests that, contrary to earlier claims,[13] polarizable carbon monoxide is not an adequate model for distal ligand effects in carbonmonoxyheme proteins and synthetic model compounds. Very probably this is caused by the large effect of the electric field on the back-bonding and the large polarizability of the π subsystem of the Fe−CO unit.

The ^{17}O shieldings of several carbonmonoxide heme models and several HbCO and MbCO at different pHs, cover a range of 21 ppm. The poor monotonic relation between $\delta(^{17}O)$ and $\nu(C-O)$ and lack of correlation between $\delta(^{17}O)$ and $\delta(^{13}C)$ show that the C−O π-bond order is not the primary factor influencing $\delta(^{17}O)$. $\delta(^{17}O)$ does not correlate with any single structural property of the Fe−CO unit, however, atropisomerism and increased deformation (ruffling) of the porphyrin geometry appear to play a significant role.

The results presented here do not provide support for recent suggestions[11a,12a,13−15] that there is a common electronic origin of both carbon-13 and oxygen-17 shieldings and clearly suggest that a reassessment of the relative importance of weak electrostatic interactions within the heme pocket and of the porphyrin skeleton distortions is needed.

Acknowledgment. This research was supported by the Greek General Secretariat of Research and Technology, FEBS (short-term fellowship to C.G.K.), and the Greek Scholarship Foundation (Ph.D. research fellowship to C.G.K.). We thank the EU-Large Scale PARABIO Facility (Contract No. 950033) at the University of Florence (Italy) for the use of the Bruker AVANCE 600 MHz instrument and Bruker-Spectrospin (Lisses, France) for the use of the Bruker AVANCE 300 MHz instrument.

IC9814165